

# THE CREST REACTIVE BURN MODEL

Caroline A. Handley

AWE Aldermaston, Reading, Berkshire, RG7 4PR, UK

**Abstract.** CREST is a new reactive-burn model that is able to reproduce a range of shock-initiation behaviour in conventional plastic bonded explosives. It uses entropy-, rather than pressure-, dependent reaction rates, allowing sustained-single-shock, double-shock and thin-pulse shock initiation experiments to be simulated with one set of parameters and without recourse to a separate 'desensitisation' model for double shocks.

## INTRODUCTION

A wealth of experimental data using the embedded particle velocity gauge technique has become available in recent years. This data provides a more rigorous test of reactive-burn models for shock initiation in heterogeneous explosives than Pop-plot data.

Most current reactive-burn models for conventional plastic bonded explosives use pressure-based reaction rates fitted to Pop-plot data. They require bolt-on 'desensitisation' models to account for multiple-shock situations and may have numerous adjustable parameters.

Many reactive-burn models are based on an ignition and growth concept. Microstructural mechanisms of ignition (hotspot formation) are linked to growth terms, often based on flame spread theories.

CREST is a new continuum reactive-burn model. It does not seek to model microstructural effects but its terms are based on recent analysis of particle-velocity gauge data for the shock to detonation transition in heterogeneous explosives. This analysis<sup>1,2</sup> indicates that reaction rates depend only on local shock strength and suggests that a function of entropy of the unreacted explosive might be an appropriate variable representing shock strength for use in reactive-burn models.

CREST is able to simulate a range of shock-initiation behaviour with one set of relatively few parameters. The use of an entropy-dependent reaction rate means that no additional 'desensitisation' model for multiple shocks is required.

In this paper, the model is fitted to particle-velocity-gauge data<sup>3</sup> for the HMX-based explosive EDC37.

## EXPERIMENTAL DATA

TABLE 1. EDC37 Shock Initiation Shots

Shot	Impactor	Impact velocity (km/s)	Input pressure (GPa)
1267	Sapphire	0.487	2.76
1160	Vistal	0.608	3.52
1122	Vistal	0.682	3.95
1120	Vistal	0.809	4.91
1159	Vistal	0.918	5.92
1277	Sapphire	1.403	10.8
1175/6	KelF/Sapphire	0.921	2.94,6.20
1194/5	KelF/Sapphire	1.170	3.93,8.58
1281/2	KelF/Sapphire	1.217	4.15,9.06
1279/ 1280	1mm KelF	1.321	4.45

Winter and Gustavsen et al.<sup>3</sup> used embedded particle velocity gauges to measure the shock initiation behaviour in EDC37. The experiments are summarised in Table 1.

Shots 1267 to 1277 were sustained-single-shock experiments, 1175 to 1282 were double-shock shots and 1279/80 were thin-pulse experiments.

## THE MODEL

CREST uses the ISE equation of state<sup>4</sup>, with a finite strain equation of state<sup>5</sup> for the solid unreacted explosive and a JWL equation of state for the gaseous reaction products. It assumes that the solid and gaseous components of the reacting explosive are in pressure equilibrium.

Total reaction rate,  $\dot{\lambda}$ , for the current model is given by the weighted sum of a fast reaction rate,  $\dot{\lambda}_1$ , and a slow reaction rate,  $\dot{\lambda}_2$ :

$$\dot{\lambda} = m_1 \dot{\lambda}_1 + m_2 \dot{\lambda}_2 \quad (1)$$

where  $m_1$  and  $m_2$  are weighting factors and will be discussed further below.

The reaction rates  $\dot{\lambda}_1$  and  $\dot{\lambda}_2$  are based on work by Lambourn<sup>1</sup>. Analysis of particle-velocity gauge data for the shock to detonation transition in heterogeneous explosives (specifically PBX 9501) showed that, in the early stages of the growth to detonation, the trajectory of peak particle velocity runs parallel to the shock trajectory, as if the reaction on any particle path is independent of its neighbours. This suggests that the reaction rate at any point is a function of time since the shock passed,  $t$ , and is limited by a depletion term  $(1 - \lambda)$ .

The fast and slow reaction rates are controlled by parameters  $b_1$  and  $b_2$  which largely determine the time of the peak reaction rate, and the slow reaction rate is proportional to the extent of the fast reaction, as shown in equations (2) and (3).

$$\dot{\lambda}_1 = b_1 t (1 - \lambda_1) \quad (2)$$

$$\dot{\lambda}_2 = b_2 t \lambda_1 (1 - \lambda_2) \quad (3)$$

Assuming  $b_1$  and  $b_2$  are constant, we can integrate (2) to give  $\lambda_1(t)$ . This allows  $t$  to be eliminated from (2). Substituting for  $\lambda_1$  allows (3) to be integrated, giving  $\lambda_2(t)$ . Rearranging,  $t$  can

be eliminated from (3), resulting in the following reaction-rate equations.

$$\dot{\lambda}_1 = [-2b_1 \ln(1 - \lambda_1)]^{1/2} (1 - \lambda_1)$$

$$\dot{\lambda}_2 = \left[ 2b_2 \left( \frac{b_2 \lambda_1}{b_1} - \ln(1 - \lambda_2) \right) \right]^{1/2} \lambda_1 (1 - \lambda_2)$$

As will be discussed below,  $b_1$  and  $b_2$  are functions of entropy of the shocked but unreacted explosive and so, although they are constant between shocks, they can change in a step-like manner when the explosive is shocked. Since it was assumed that  $b_1$  and  $b_2$  are constant, the derivation is not mathematically rigorous. Nevertheless, we use the above reaction-rate equations in CREST because they were found to be adequate for modelling the shock to detonation transition in EDC37.

The time-dependence of these reaction-rate equations is illustrated in Fig. 1.

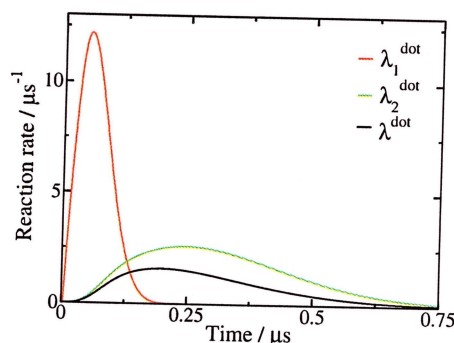


FIGURE 1. Typical CREST reaction rates (from a gauge positioned near the vial-EDC37 interface in a simulation of shot 1159).

## FITTING METHOD

Analysis of particle-velocity gauge data for the shock to detonation transition in heterogeneous explosives<sup>1,2</sup> indicates that reaction rates might depend only on local shock strength. It has been suggested<sup>2</sup> that a function of entropy of the unreacted explosive,  $Z_S$ , (which is constant between shocks) might be the most appropriate representing shock strength for use in reaction rates. In CREST,  $Z_S$  is calculated within the finite strain equation of state<sup>5</sup> for the unreacted explosive.

The form of the parameters  $b_1$  and  $b_2$  is suggested by the experimental data. A plot of the difference between the time of peak particle velocity and the time of shock arrival at each gauge, against the particle velocity at the shock (which can be related to the entropy function  $Z_S$ ), is approximately linear on a log scale<sup>2</sup> as sketched in Fig. 2.

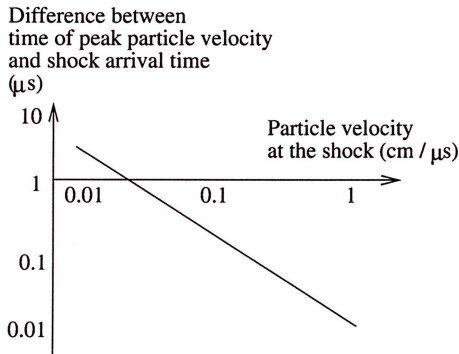


FIGURE 2. Experimental observation<sup>2</sup> that suggests a power-law form for  $b(Z_S)$ .

Since the time of peak reaction rate is believed to be close to the time of peak particle velocity<sup>1</sup>, and the time of peak reaction rate in CREST is controlled by the  $b$  parameters (it decreases as  $b$  increases), this relationship suggests a power-law form for  $b(Z_S)$ :

$$b_1 = c_0(Z_S)^{c_1} \quad b_2 = c_2(Z_S)^{c_3} \quad (4)$$

Using equation (2), it can be shown that the magnitude of the peak reaction rate is proportional to both  $m$  and  $\sqrt{b}$ . To remove the dependence on  $b$ , the expressions for  $m_1$  and  $m_2$  contain a factor of  $b^{-1/2}$ , as shown in equation (5). A factor of  $(1-\lambda)$  is included because, during the fitting process, it was found to be necessary to have  $m_2 > 1$  for some values of  $Z_S$ , so  $\lambda$  reached one before  $\lambda_2$  did and, more importantly, before  $\lambda_2$  had fallen to zero. This meant that  $\lambda$  contained a discontinuity which caused unphysical perturbations to the flow. Incorporating a factor of  $(1-\lambda)$  in the expressions for  $m$  (5), ensures that  $\lambda$  is a smoothly-varying function of time.

The remaining factors controlling  $m_1$  and  $m_2$  were chosen by trial and error, by observing the effect of changes in the reaction-rate parameters on the simulated particle-velocity histories.

$$m_1 = \frac{c_6}{\sqrt{b_1}}(1-\lambda) \quad (5)$$

$$m_2 = \left[ \frac{c_8(Z_S)^{-c_9} + c_{10}(Z_S)^{c_{11}}}{\sqrt{b_2}} \right] (1-\lambda)$$

A one-dimensional Lagrangian finite-difference multi-material hydrocode PERUSE<sup>6</sup> was used to simulate the experimental data. CREST parameters were chosen to fit sustained-single-shock shots 1267, 1160, 1159 and 1277 simultaneously and are listed in Table 2.

TABLE 2. CREST parameters for EDC37.

$\rho_0$	1.8445	g/cm <sup>3</sup>
Reaction products equation of state		
$A$	6.642021	Mbar
$B$	0.2282927	Mbar
$R_1$	4.25	
$R_2$	1.825	
$\omega$	0.25	
Unreacted equation of state		
$Q$	0.0719557	Mbar cm <sup>3</sup> /g
$K_{0S}$	0.1424525	Mbar
$A_1$	2.417494	
$A_2$	2.208027	
$A_3$	0	
$\Gamma_1$	32.33557	
$\Gamma_2$	3.596933	
$\chi_{00}$	0.4	
$m$	2.0	
$T_{0S}$	293.0	K
$C_{v0S}$	$9.17 \times 10^{-6}$	Mbar cm <sup>3</sup> /g K
$dC_{vS}/dT$	0.0	Mbar cm <sup>3</sup> /g K <sup>2</sup>
Reaction rate parameters		
$c_0$	$2.0 \times 10^8$	$\mu\text{s}^{-2}(\text{Mbar cm}^3/\text{g})^{-c_1}$
$c_1$	2.0	
$c_2$	$2.2 \times 10^8$	$\mu\text{s}^{-2}(\text{Mbar cm}^3/\text{g})^{-c_3}$
$c_3$	2.5	
$c_6$	0.0	$\mu\text{s}^{-1}$
$c_8$	$1.6 \times 10^{-4}$	$\mu\text{s}^{-1}(\text{Mbar cm}^3/\text{g})^{c_9}$
$c_9$	1.0	
$c_{10}$	$4.0 \times 10^5$	$\mu\text{s}^{-1}(\text{Mbar cm}^3/\text{g})^{-c_{11}}$
$c_{11}$	1.8	

Constants  $c_4$ ,  $c_5$ ,  $c_7$  and  $c_{12}-c_{15}$  were included in the PERUSE coding but are not used in the EDC37 fit described here.

The forms of  $m_2$ ,  $b_1$  and  $b_2$  with the relevant fitting constants are shown in Fig. 3a and Fig. 3b. Note that  $m_1 = 0$ , so  $\dot{\lambda}$  does not depend directly on  $\dot{\lambda}_1$ . However, the slow reaction rate  $\dot{\lambda}_2$  depends on the extent of the fast reaction  $\dot{\lambda}_1$  and so we can not dispense with the fast reaction altogether. Effectively, the fast reaction acts as a switch that ensures that  $\dot{\lambda}$  is initially cubic in time (see Fig. 1).

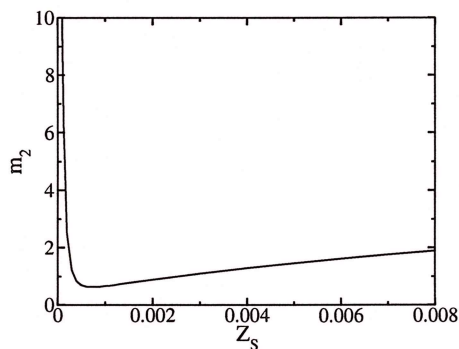


FIGURE 3a. Dependence of  $m_2$  on  $Z_s$ .

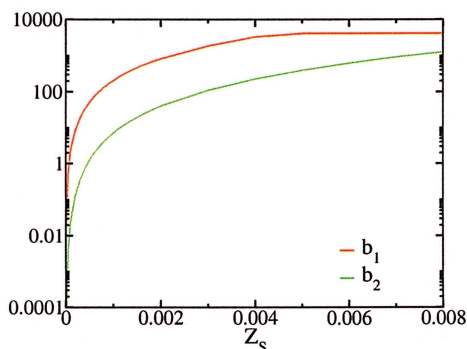


FIGURE 3b. Dependence of  $b_1$  and  $b_2$  on  $Z_s$ .

A limit is introduced in the CREST coding to prevent  $b_1$  and  $b_2$  exceeding 4000 and to prevent  $m_2$  exceeding 10. These prevent reaction run-away and increase code robustness.

Particle-velocity histories from the CREST simulations are shown with the experimental data in Fig. 4 to 9 and 11. Only selected traces from each shot are displayed for ease of viewing.

The sustained-single-shock simulations used a 3cm-thick sapphire or vialist impactor incident at

the experimental impact velocity upon an EDC37 target, also 3cm thick. This geometry is not representative of the exact experimental configuration which explains why the rarefactions observed in the experimental traces for shots 1267 and 1160 are not seen in the computational fit. Use of an inexact geometry is not thought to influence the quality of the CREST fit to the experimental results.

For the double-shock shots, the impactor consisted of a ~1mm-thick Kelf sheet backed with 3cm of sapphire, whereas for the thin-pulse shot, a 1mm-thick Kelf sheet was incident on 3cm of EDC37. Scalar monotonic artificial viscosity was used for the simulations. Computational gauges were placed as close as possible to the experimental locations.

## DISCUSSION

### Fit to sustained-single-shock experiments

The CREST fits to sustained-single-shock shots 1267 to 1277, illustrated in Fig. 4 to 7, are qualitatively good. The time of shock arrival is well matched, as is the time of peak particle velocity. The shape of the computational particle-velocity histories is similar to the experimental traces and, in most cases, a reasonable fit to shock strength (i.e. particle velocity at the time of shock arrival) and magnitude of peak particle velocity is obtained.

It should be emphasised that this fit uses one set of coefficients  $c_0 - c_{11}$  for all the experimental shots; variation of reaction rates to match shots of different input pressure is achieved by using reaction-rate parameters  $m_1$ ,  $m_2$ ,  $b_1$ , and  $b_2$  dependent on simple functions of entropy, with coefficients  $c_0 - c_{11}$ .

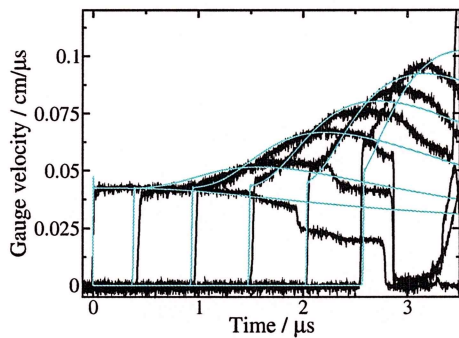


FIGURE 4. Fit to shot 1267 (light green traces) using CREST. Experimental (black traces) input pressure 2.76GPa.

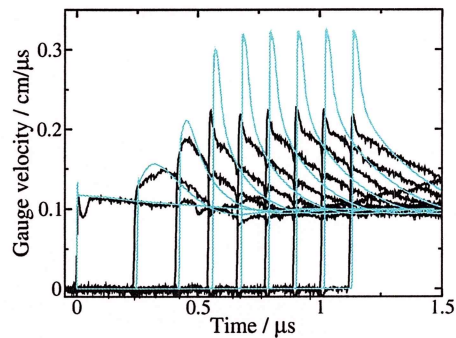


FIGURE 7. Fit to shot 1277 (light green traces) using CREST. Experimental (black traces) input pressure 10.8GPa.

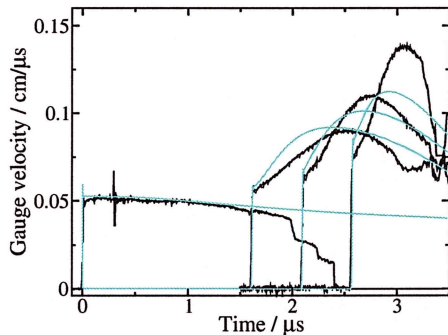


FIGURE 5. Fit to shot 1160 (light green traces) using CREST. Experimental (black traces) input pressure 3.52GPa. Fits to shots 1122 and 1120 (not shown) are similar to these.

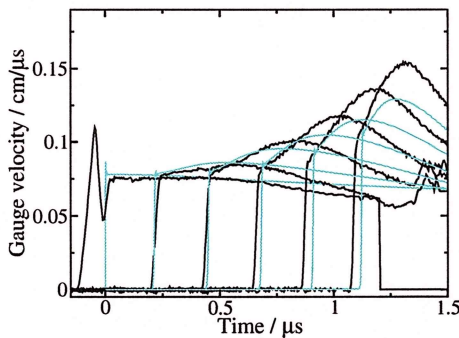


FIGURE 6. Fit to shot 1159 (light green traces) using CREST. Experimental (black traces) input pressure 5.92GPa.

#### Fit to double-shock and thin-pulse shots

The CREST fit to double-shock shots 1175/6 and 1194/5, illustrated in Fig. 8 and 9, is reasonable. No bolt-on 'desensitisation' model is necessary to model multiple-shock situations, in contrast to many pressure-dependent models. This advantage is achieved by using an entropy-based reaction-rate. In a double-shock situation, the internal energy (and therefore entropy) reached in the target by a double shock up to pressure  $p$  is considerably less than that reached by a single shock to the same pressure. This is illustrated in Fig. 10 and means that the reaction rate in an entropy-based model will be very different to that predicted with a pressure-dependent model.

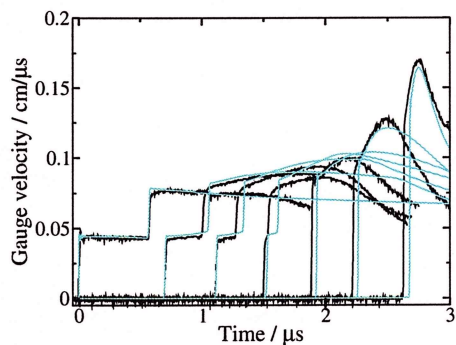


FIGURE 8. Fit to shot 1175/6 (light green traces) using Lee-Tarver (above) and CREST (below). Experimental (black traces) input pressures 2.94GPa and 6.2GPa.

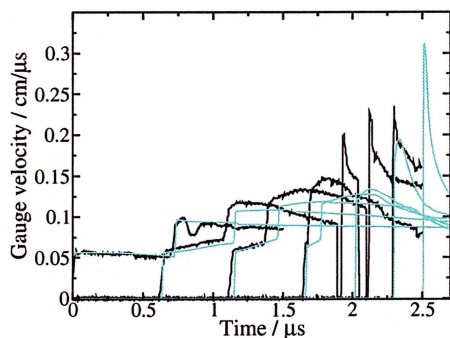


FIGURE 9. Fit to shot 1194/5 (light green traces) using CREST. Experimental (black traces) input pressures 3.93GPa and 8.58GPa. Fit to shot 1281/2 (not shown) is not dissimilar to this.

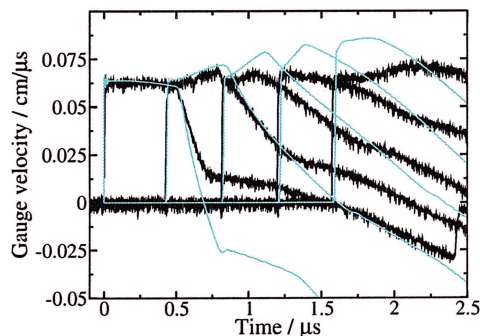


FIGURE 11. Fit to shot 1279 (light green traces) using CREST. Experimental (black traces) input pressure 4.45GPa.

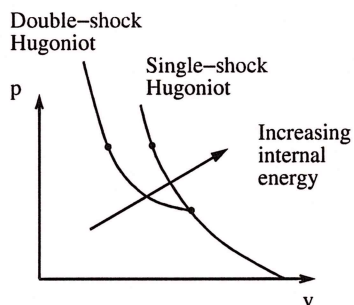


FIGURE 10. Entropy reached in double and single-shock situations. Since entropy (with internal energy) increases in the direction shown, a piece of explosive which has been single-shocked to a given pressure will have a higher entropy than a piece which has been double-shocked to the same pressure.

The CREST fits to the double-shock and thin-pulse (Fig. 11) shots are clearly not perfect. For the double shock, there is some difficulty in modelling the time of arrival of the second shock and the detailed shape of the post-second-shock particle velocity histories. Similarly, for the thin-pulse shot, the time of arrival of the tail of the rarefaction wave from the rear surface of the flyer is not accurately matched. These problems indicate that the equations of state require improvement.

## CONCLUSIONS

The CREST reaction-rate model described above provides a reasonable fit to a variety of EDC37 gas-gun experiments, using one set of coefficients to match shots ranging in shock strength between 2.7 and 10.8 GPa.

CREST allows sustained-single-shock, double-shock and thin-pulse experiments to be simulated without the need for a separate 'desensitisation' model. This is because CREST uses entropy-dependent reaction-rates whereas most reactive-burn models use pressure dependency. It is our belief that the phenomenon known as 'desensitisation' for double-shocks is simply a manifestation of using pressure-dependent models, rather than being a physical effect.

Since they rely on internal energy calculations, entropy-dependent models suffer from a number of computational problems. These will be discussed in another paper<sup>7</sup>. It is our belief that the advantages associated with the use of entropy-based reaction rates outweigh the disadvantages.

## REFERENCES

1. Lambourn, B.D., "An Interpretation of Particle Velocity Histories during Growth to Detonation", *Shock Compression of Condensed Matter-2003*, AIP Conference Proceedings 706, New York, pp. 367-370, 2004.
2. James, H.R., and Lambourn, B.D., "On the systematics of particle velocity histories in the shock to detonation transition regime", accepted for publication in *J. Appl. Physics*, 2006.
3. Winter, R.E., Sorber, S.S., Salisbury, D.A., Taylor, P., Gustavsen, R., Sheffield, S., Alcon, R., "Experimental Study of the Shock Response of an HMX-based Explosive", *Shock Waves*, Published Online at [www.springer.com](http://www.springer.com), Online Reference: DOI:10.1007/s00193-006-0006-5, 2006.
4. Cowperthwaite, M., "A Constitutive Model for Calculating Chemical Energy Release Rates from the Flow Fields in Shocked Explosives", *Proceedings of the 7<sup>th</sup> Detonation Symposium*, pp. 498-505, 1981.
5. Lambourn, B.D., "A Complete EOS for Non-Reacted Explosives", to appear in *Shock Compression of Condensed Matter-2005*, AIP Conference Proceedings.
6. Whitworth, N.J., "Simple One-Dimensional Model of Hot-Spot Formation in Heterogeneous Solid Explosives", *Numerical Methods & Software Systems: MSc Dissertation*, Royal Military College of Science, Cranfield University, 1999
7. Whitworth, N.J., "Some Issues Regarding the Hydrocode Implementation of the CREST Reactive Burn Model", this proceedings.